Author Manuscript

Author Manuscript

Author Manuscript

Author Manuscript

HHS Public Access

Author manuscript

ACS Chem Neurosci. Author manuscript; available in PMC 2022 May 17.

Published in final edited form as:

ACS Chem Neurosci. 2022 March 02; 13(5): 688–699. doi:10.1021/acschemneuro.1c00854.

Small molecules targeting PTPσ—Trk interactions promote sympathetic nerve regeneration

Matthew R. Blake[1,2,#], **Ryan T. Gardner**[1,5,#], **Haihong Jin**[1,6], **Melanie A. Staffenson**[1], **Nicole J. Rueb**[3], **Amy M. Barrios**[3], **Gregory B. Dudley**[4], **Michael S. Cohen**[1], **Beth A. Habecker**[1]

[1]Department of Chemical Physiology and Biochemistry, Oregon Health and Science University, Portland, OR 97239, USA

[2]Graduate Program in Biomedical Sciences, Oregon Health and Science University, Portland, OR 97239, USA

[3]Department of Medicinal Chemistry, University of Utah College of Pharmacy, Salt Lake City, UT 84112, USA

[4]C. Eugene Bennett Department of Chemistry, West Virginia University, Morgantown, WV 26506, USA

Abstract

Chondroitin Sulfate Proteoglycans (CSPGs) prevent sympathetic nerve regeneration in the heart after myocardial infarction, and prevent central nerve regrowth after traumatic brain injury and spinal cord injury. Currently there are no small molecule therapeutics to promote nerve regeneration through CSPG-containing scars. CSPGs bind to monomers of receptor protein tyrosine phosphatase sigma (PTPσ) on the surface of neurons, enhancing the ability of PTPσ to bind and dephosphorylate Trk tyrosine kinases, inhibiting their activity and preventing axon outgrowth. Targeting PTPσ—Trk interactions is thus a potential therapeutic target. Here we describe the development and synthesis of small molecules (HJ-01, HJ-02) that disrupt PTPσ interactions with tropomyosin receptor kinases (Trks), enhance Trk signaling, and promote sympathetic nerve regeneration over CSPGs.

Address for Correspondence: Beth A. Habecker PhD, Department of Chemical Physiology and Biochemistry, L334, Oregon Health and Science University, 3181 SW Sam Jackson Park Rd, Portland, OR 97239, habecker@ohsu.edu Or Michael S. Cohen PhD, Department of Chemical Physiology and Biochemistry, L334, Oregon Health and Science University, 3181 SW Sam Jackson Park Rd, Portland, OR 97239, cohenmic@ohsu.edu.

[#]Authors contributed equally

Author Contributions: MRB, RTG, BAH designed and conducted experiments, collected and analyzed data, and wrote the manuscript. MSC developed the small molecules, designed and conducted experiments and wrote the manuscript. HJ helped design and synthesize the small molecules. MS conducted experiments and analyzed data. NJR, AMB, GBD designed, conducted, analyzed phosphatase screening experiments, produced Illudalic acid and provided input on the manuscript.

[5]Current address: Ryan T. Gardner, Merz Therapeutics, 6601 Six Forks Road, suite 430, Raleigh, NC, 27615

[6]Current address: Haihong Jin, Atomwise, 717 Market St #800, San Francisco, CA 94103

Conflicts of Interest: The authors of this study have no conflicts of interest to report.

Supporting Information

The Supporting Information includes the full synthesis scheme and chemical products.

Author Manuscript Author Manuscript Author Manuscript Author Manuscript

Keywords

Chondroitin sulfate proteoglycan; protein tyrosine phosphatase receptor sigma; nerve regeneration; acrylamide

Introduction

The lack of nerve regeneration after spinal cord injury, traumatic brain injury, extremity injury, and even myocardial infarction is due, in part, to inhibitory extracellular matrix components including chondroitin sulfate proteoglycans (CSPGs). A current approach to overcoming CSPG inhibition of axon outgrowth focuses on enzymatic degradation of chondroitin sulfate side chains using chondroitinase ABC (ChABC). Intrathecal treatment with ChABC [1], local injection of the enzyme near nerve grafts [2, 3], or viral expression of modified ChABC [4] has proven successful in restoring nerve regeneration after spinal cord injury. However, the need to express or inject a functional enzyme *in vivo*, and maintain levels for an extended period of time, raises concerns about safety and applicability to humans. Recent studies identified protein tyrosine phosphatase receptor sigma (PTPσ) as a receptor for CSPGs [5], and showed that knockout of PTPσ in mice enhanced nerve regeneration after spinal cord injury [6] or myocardial infarction [7]. Likewise, modulating PTPσ activity with intracellular sigma peptide (ISP), a cell permeable peptide that disrupts PTPσ-substrate binding [8] enhanced nerve regeneration after spinal cord injury in rats [8] and restored nerve regeneration after myocardial infarction in mice [9]. Development of the therapeutic peptide was a significant milestone but no small molecule therapeutics exist to overcome CSPG inhibition of nerve regeneration.

The mechanisms by which PTPσ and homologues such as LAR (Leukocyte common antigen-related receptor) inhibit axon outgrowth are not fully understood, but interactions with Trk neurotrophin receptors (TrkA, TrkB, and TrkC) are thought to play a key role [10, 11]. PTPσ and LAR both bind to and dephosphorylate Trk receptors, inhibiting their kinase activity and decreasing axon outgrowth [11]. Removing PTPσ or disrupting phosphatase binding to Trk receptors enhances Trk signaling [10] and axon outgrowth [8, 9]. These studies suggest that inhibiting PTPσ or disrupting the interaction between PTPσ and TrkA should enhance sympathetic axon outgrowth across CSPGs.

Here, we describe small molecules (HJ-01 and HJ-02) inspired by illudalic acid, a natural product shown to inhibit PTPσ catalytic activity [12–14]. Surprisingly, HJ-01 and HJ-02 do not inhibit PTPσ activity, but instead disrupt the interaction between PTPσ and TrkA. HJ-01 and HJ-02 enhance Trk signaling and restore sympathetic axon outgrowth across CSPGs.

Results and Discussion

Design and Synthesis of a PTPσ inhibitor

We sought to identify an inhibitor of PTPσ catalytic activity and were inspired by the natural product Illudalic acid (Fig. 1) which inhibits PTPσ and the related phosphatase LAR. Illudalic acid exhibits an IC50 of <<250 nM against PTPσ catalytic activity *in vitro* [14]. Illudalic acid contains an aldehyde as well as a hemi-acetal lactone that opens up to an

Author Manuscript Author Manuscript Author Manuscript Author Manuscript

aldehyde at physiological pH; the bis-aldehyde is required for activity, presumably because it is required to form a stable covalent bond with the active site cysteine of LAR/PTPσ. Because of (i) potential cellular instability of the bis-aldehyde and (ii) the complex, multi-step synthesis of illudalic acid we envisaged a simpler analog with better physiochemical properties for in cell and *in vivo* studies. Inspired by illudalic acid and closely related analogs, we rationally designed two small molecules, HJ-01 and HJ-02 (Fig. 1). Similar to illudalic acid analogs, HJ-01 and HJ-02 are based on *p*-hydroxy benzoic acid scaffold, however, the bis-aldehyde was replaced with an acrylamide group designed to react with the catalytic cysteine in PTPσ. HJ-01 and HJ-02 could be synthesized in four steps from commercially available starting material (Scheme S1, Supporting Information).

HJ-01 and HJ-02 rescue neurite and axon outgrowth over CSPGs

CSPGs are potent inhibitors of central and peripheral neuron outgrowth. The primary CSPG receptor in sympathetic neurons is PTPσ, and deleting PTPσ or disrupting PTPσ-substrate interactions with ISP enhances sympathetic axon growth across CSPGs [7, 9]. We asked if our small molecules could restore sympathetic axon outgrowth over inhibitory CSPGs, performing live cell imaging of neurons grown on plates coated with laminin or a combination of laminin and CSPGs. Additional cells were treated with HJ-03, a structural analog of HJ-01 and HJ-02 in which the acrylamide was replaced with a non-reactive ethylamide isostere (Scheme S1, Supporting Information), illudalic acid, or ISP. CSPGs significantly limited axon outgrowth as expected, and HJ-01 and HJ-02 restored axon outgrowth in a dose dependent manner (Figure 2). HJ-01 and HJ-02 fully restored growth at 100 nM. ISP also restored axon growth over CSPGs at 1 μM, but HJ-03 and illudalic acid did not (Figure 2). These results show that HJ-01 and HJ-02 promote sympathetic axon outgrowth across CSPGs, and their activity is dependent on the acrylamide electrophile, consistent with covalent inhibition.

CSPGs inhibit axon outgrowth *in vivo* through interaction with the distal axon. To confirm that these compounds acted on axons, we cultured sympathetic neurons in microfluidic chambers to separate the cell bodies from the axons, with treatments confined to the axon compartment. The distal axon compartment was coated with either collagen or collagen and CSPGs prior to adding neurons. After axons had extended into the distal compartment, the axon compartment was treated for 3 hours with vehicle (5% DMSO), 100 nM HJ-01, 100 nM HJ-02, or 4 μU/mL chondroitinase ABC as a positive control to disrupt CSPGs. Acute treatment with the small molecules (Figure 3) or the positive control chondroitinase ABC (data not shown) stimulated the defasiculation of axon bundles growing over CSPGs and enhanced the rate of axon outgrowth. These results suggest HJ-01 and HJ-02 target axons to promote outgrowth across CSPGs.

HJ-01 and HJ-02 do not inhibit phosphatase activity

Based on the mechanism of action of illudalic acid, we hypothesized that HJ-01 and HJ-02 would irreversibly inhibit the catalytic activity of PTPσ by reacting with the active site cysteine in the D1 catalytic domain via a Michael addition with their acrylamide. To test the hypothesis that these compounds inhibit PTPσ D1 catalytic activity, we expressed and purified a peptide including the D1 domain and the inactive D2 pseudocatalytic

Author Manuscript Author Manuscript Author Manuscript Author Manuscript

domain. We used the compound p-nitrophenol phosphate (p-NPP) to monitor phosphatase activity through a colorimetric reaction. We incubated D1D2 peptide with either vehicle (5% DMSO), 1 μM HJ-02, or the phosphatase inhibitor orthovanadate (10 mM) as a negative control in the presence of either 2 mM or 10 mM p-NPP. HJ-02 did not inhibit D1 phosphatase activity at 1 μM concentration, even though lower doses restored axon outgrowth *in vitro*. Samples treated with orthovanadate had negligible phosphatase activity as expected (Figure 4A,B). We also tested higher doses of HJ-01 and HJ-02 against a panel of protein phosphatases and found minimal inhibition of phosphatase activity with 100 μM HJ-01 or HJ-02 (Figure 4C,D), which is three orders of magnitude higher than the dose needed to restore axon outgrowth. These results show that HJ-01 and HJ-02 do not inhibit the catalytic activity of PTPσ at biologically relevant concentrations and conditions and suggest that they affect PTPσ function via a different mechanism. In contrast, illudalic acid fully inhibited PTPσ activity at 1 μM (Figure 4E) but had no effect on axon outgrowth at concentrations up to 10 μM.

HJ-01 and HJ-02 disrupt TrkA—PTPσ interactions

Interaction of PTPσ with its protein substrates is required for efficient dephosphorylation. Trk tyrosine kinase receptors are critical substrates of PTPσ in neurons, and disrupting PTPσ binding to Trk receptors enhances Trk signaling [10] and axon outgrowth [8, 9]. Thus, we asked if HJ-01 and HJ-02 altered the interaction between PTPσ and TrkA, the Trk receptor present in sympathetic neurons.

We transfected HEK 293T cells with PTPσ and TrkA tagged with red fluorescent protein (TrkA-RFP), and examined the ability of HJ-01 and HJ-02 to disrupt TrkA—PTPσ binding. Cells were treated with vehicle (DMSO), HJ-01, HJ-02, or the biologically inactive compound HJ-03 and were stimulated simultaneously with NGF and CSPGs. These conditions were used to mimic the environmental conditions present during sympathetic nerve regeneration in our experimental model. We immunoprecipitated TrkA-RFP using an RFP-nanobody and compared the PTPσ pulled down following HJ-01 or HJ-02 treatment (100 nM and 1 μM) with the amount pulled down in vehicle treated cells. The small molecules HJ-01 and HJ-02 disrupted TrkA—PTPσ interactions as measured by pulldown efficiency, while the biologically inactive structural analog, HJ-03, did not disrupt TrkA—PTPσ binding (Figure 5A–C). To further test the specificity of these compounds, we asked if HJ-02 disrupted TrkA interactions with the p75 neurotrophin receptor (p75NTR), which together form the high-affinity binding site for NGF. Addition of HJ-02 did not alter the ability of TrkA-RFP to pull down p75NTR (Figure 5D), suggesting selectivity for disrupting TrkA—PTPσ interactions. These data support the model that HJ-01 and HJ-02 promote axon outgrowth by disrupting the interaction between PTPσ and TrkA, but the concentration required to break Trk—PTP complexes was higher than the concentration that restored axon outgrowth. This suggests that HJ-01 and HJ-02 modulate Trk—PTPσ interactions and subsequent Trk signaling at lower concentrations than are necessary to significantly disrupt Trk—PTPσ complexes.

Author Manuscript Author Manuscript Author Manuscript Author Manuscript

HJ-01 and HJ-02 reverse PTPσ-inhibition of Trk signaling

PTPσ dephosphorylates Trk receptors [11] and the absence of PTPσ enhances Trk signaling, noted by increased phosphorylation of downstream signaling proteins including ERK1/2 and Akt [15]. To determine if disruption of Trk—PTPσ complexes by HJ-01 and HJ-02 prevented PTPσ inhibition of Trk signaling, we used HEK 293T cells stably expressing TrkB (HEK-TrkB). Co-expression of full-length PTPσ in HEK-TrkB cells decreased BDNF-induced ERK1/2 phosphorylation, and addition of HJ-01 or HJ-02 restored ERK1/2 phosphorylation to normal BDNF-stimulated levels (Figure 6A,B). Similar to the neurite outgrowth data in TrkA-expressing sympathetic neurons, HJ-02 was slightly more potent than HJ-01 in rescuing PTPσ-suppressed ERK1/2 phosphorylation. Likewise, both compounds restored ERK phosphorylation at 100 nM, consistent with the dosing that restored axon outgrowth in neurons, but lower than the dose needed to significantly disrupt TrkA—PTPσ binding in pull-down experiments. Taken together these results support the notion that HJ-01 and HJ-02 prevent PTPσ-mediated dephosphorylation of Trk receptors by modulating the interaction between PTPσ and Trks. Since HJ compounds did not inhibit PTPσ activity, but did inhibit downstream signaling, we asked if HJ-01 or HJ-02 disrupted signaling downstream from tyrosine phosphatase PTP1B and its substrate the insulin receptor (IR-β) [16]. Both receptors are present in the human hepatic cell line HepG2. Insulin stimulation of IR-β in HepG2 cells increased phosphorylation of ERK1/2, and inhibiting PTP1B with CinnGel 2ME further enhanced ERK signaling. Conversely, HJ-01 and HJ-02 had no effect on ERK1/2 phosphorylation in insulin-stimulated HepG2 cells, indicating they do not disrupt PTP1B dephosphorylation of IR-β (Figure 6C,D).

Discussion

There is a great need for therapeutics that can facilitate axon regeneration and cell migration through CSPG-laden scar tissue. Small molecules that promote axon outgrowth through inhibitory environments are promising therapeutics for spinal cord injury, traumatic brain injury, or myocardial infarction [5, 8, 9, 17]. In this study, we synthesized two natural product-inspired, acrylamide-based compounds, HJ-01 and HJ-02, which were designed to covalently inactivate PTPσ activity. HJ-01 and HJ-02, restored axon outgrowth across inhibitory CSPGs *in vitro*. A compound (HJ-03) lacking an acrylamide had no biological activity, suggesting that covalent binding was important for function. Our experiments with primary neurons found no evidence of non-specific binding or toxicity. Importantly, there are several examples of FDA approved drugs (e.g. BTK inhibitor, Ibrutinib) that contain acrylamides, demonstrating that compounds with this type of electrophile are effective *in vivo*.

PTPσ regulation of axon dynamics depends on its ability to bind to and dephosphorylate substrate proteins including Trk tyrosine kinases [11]. Modulation of substrate binding can occur through two distinct mechanisms, one extracellular and one intracellular. Extracellular CSPGs bind to PTPσ monomers, which can then bind to and dephosphorylate substrate proteins like Trk receptors, decreasing axon outgrowth. In contrast, extracellular heparin sulfate proteoglycans (HSPGs) stimulate oligomerization of PTPσ into aggregates sequestered from Trk receptors, promoting axon outgrowth [18]. Intracellular binding of peptides like ISP or small molecules to the D2 pseudocatalytic domain of PTPσ can also

Author Manuscript Author Manuscript Author Manuscript Author Manuscript

disrupt substrate binding and enhance axon outgrowth [10]. Unexpectedly, we found that HJ-01 and HJ-02 did not block PTPσ phosphatase activity, but rather modulated PTPσ—Trk receptor signaling, and at higher doses disrupted the PTPσ—Trk complex. Interestingly, the PTPσ inhibitor illudalic acid did not rescue axon outgrowth, in distinct contrast to ISP, HJ-01, and HJ-02 which do not inhibit the phosphatase but modulate PTPσ—Trk interactions. The disruption of the interaction between PTPσ—TrkA by HJ-01 and HJ-02 in a cysteine-dependent manner may be similar to the disruption of IRAK4—MyD88 interactions by the multiple sclerosis drug dimethyl fumarate (DMF) [19]. These results suggest that HJ-01 and HJ-02 elicit their effects via altering PTPσ—Trk interactions by covalently binding to either PTPσ or Trk; however, due to the lack of direct binding data, we cannot rule out that HJ-01 and HJ-02 bind to an unidentified protein involved in PTPσ—Trk complex formation.

We generated novel small molecules designed to target PTPσ in order to promote nerve regeneration through CSPG-containing scars. Two compounds that we generated restore nerve growth *in vitro* at nanomolar concentrations. Although our focus was on sympathetic neurons, CSPGs in the glial scar inhibit nerve regeneration after traumatic brain injury and spinal cord injury, preventing cognitive or motor recovery [17]. CSPG-PTPσ interactions also disrupt myelin repair in multiple sclerosis by inhibiting oligodendrocyte precursor cell (OPC) migration into demyelinated regions and preventing differentiation of OPCs into oligodendrocytes [20–22]. HJ-01 and HJ-02 may prove useful for ameliorating disease progression in these situations. Small molecules are simpler to produce and easier to administer than the peptide (ISP) and enzyme (chondroitinase ABC)-based strategies that are the primary current focus of therapeutic development. Thus, HJ-01 and HJ-02 are an important advance in the development of therapies designed to overcome CSPG actions.

Methods

General Chemistry methods.

General.—^{1}H NMR were recorded on a Bruker DPX spectrometer at 400 MHz. Chemical shifts are reported as parts per million (ppm) downfield from an internal tetramethylsilane standard or solvent references. Solvents for reactions were dried using a solvent purification system manufactured by Glass Contour, Inc. (Laguna Beach, CA) unless otherwise indicated. Triethylamine (Et_3N) was stored over NaOH. All other solvents were of ACS chemical grade (Fisher Scientific) and used without further purification unless otherwise indicated. Reagents were of ACS chemical grade (Fisher Scientific) and used as received.

Methyl 5-(cyclohexylmethoxy)-4-methoxy-2-nitrobenzoate (2-1)—To a solution of methyl 5-hydroxy-4-methoxy2-nitrobenzoate (227 mg, 1.0 mmol) in DMF (10 ml) was added K_2CO_3 (207 mg, 1.5 mmol) and cyclohexylmethyl bromide (212 mg, 1.2 mmol). The reaction mixture was heated to 100°C and stirred for 10 h. After the reaction was over, the mixture was cooled to room temperature RT). The mixture was then filtered to remove the inorganic material. Filtrate was diluted with water (5 ml) and extracted with ethyl acetate (3x10 ml). The combined organic layers were washed with water (3x10 ml) and dried over anhydrous sodium sulfate. Removal of solvent under vacuo gave the residue which was

Author Manuscript Author Manuscript Author Manuscript Author Manuscript

chromatographed on silica gel with EtOAc : Hexane (1:4 v/v) as eluent to give 293 mg (yield 91%) of the desired product. ^{1}H NMR (400 MHz, Chloroform-*d*) δ ^{1}H NMR (400 MHz, Chloroform-*d*) δ 7.44 (s, 1H), 7.02 (s, 1H), 3.94 (s, 3H), 3.89 (s, 3H), 3.87 (d, *J* = 6.3 Hz, 2H), 1.87-1.74 (m, 6H), 1.37 – 1.14 (m, 3H), 1.12 – 0.90 (m, 2H). ^{13}C NMR (101 MHz, $CDCl_3$) δ 166.62, 152.60, 150.69, 140.80, 121.85, 111.67, 107.23, 75.09, 56.66, 53.33, 37.37, 29.83, 26.46, 25.70.

Methyl 2-amino-5-(cyclohexylmethoxy)-4-methoxybenzoate (3-1)—To a solution of methyl5-(cyclohexylmethoxy)-4-methoxy-2-nitrobenzoate (**2**) (260 mg, 0.80 mmol) in anhydrous MeOH was added Pd/C (10 wt%, 55 mg). The mixture was stirred under H_2 atmosphere for 4 h before it was filtered through a pad of celite. The solvent was removed in vacuo and the residue was purified by flash column chromatography to afford 218 mg (93%) of the desired product. ^{1}H NMR (400 MHz, Chloroform-*d*) δ 7.29 (s, 1H), 6.12 (s, 1H), 5.57 (s, 2H), 3.88 (s, 3H), 3.83 (s, 3H), 3.71 (d, *J* = 6.4 Hz, 2H), 1.91-1.69 (m, 6H), 1.34 - 1.15 (m, 3H), 1.01 (m, 2H).^{13}C NMR (101 MHz, $CDCl_3$) δ 168.30, 155.67, 147.22, 140.33, 115.21, 102.23, 99.50, 75.66, 55.83, 51.40, 37.76, 30.09, 26.68, 25.88

Methyl 2-acrylamido-5-(cyclohexylmethoxy)-4-methoxybenzoate (4-1)—Methyl 2-amino-5-(cyclohexylmethoxy)-4-methoxybenzoate **(3)** (205 mg, 0.70 mmol) was dissolved in DCM (5 ml) followed by addition of acryloyl chloride (76 mg, 0.84 mmol) at 0°C. Triethylamine (84 mg, 0.84 mmol) was then syringed into the reaction mixture and the solution was stirred for 4 h and allowed to warm to RT. The reaction was concentrated and re-dissolved in EtOAc. The organic solution was then washed with water, saturated sodium bicarbonate, and brine. The organic layer was dried over magnesium sulfate, filtered, concentrated, and purified by column chromatography (1:4) EtOAc:Hexanes) to deliver 221 mg (yield 91%) of the desired product. ^{1}H NMR (400 MHz, Chloroform-*d*) δ 11.39 (s, 1H), 8.56 (s, 1H), 7.44 (s, 1H), 6.41-6.24 (m, 2H), 5.77 (dt, *J* = 10.0, 1.6 Hz, 1H), 3.95 (s, 3H), 3.93(s, 3H), 3.77 (dd, *J* = 6.4, 1.8 Hz, 2H), 1.96 – 1.64 (m, 6H), 1.38 – 1.11 (m, 3H), 1.11 – 0.96 (m, 2H). ^{13}C NMR (101 MHz, $CDCl_3$) δ 168.67, 164.16, 154.75, 143.92, 137.66, 132.53, 127.28, 114.11, 106.74, 75.00, 56.22, 52.25, 37.68, 30.08, 26.65, 25.86.

2-Acrylamido-5-(cyclohexylmethoxy)-4-methoxybenzoic acid (5-1, HJ-01)—Methyl 2-acrylamido-5-(cyclohexylmethoxy)-4-methoxybenzoate (**4-1**) (20 mg, 0.06 mmol) was dissolved in THF (1mL) followed by 2 M LiOH (0.12 ml, 0.24 mmol) and the mixture was stirred at RT overnight. After the reaction was over, acidify the mixture with 1N HCl and the product was extracted with ethyl acetate to afford 16 mg. Yield: 85%.

^{1}H NMR (400 MHz, Chloroform-d) δ 8.46 (s, 1H), 7.55 (s, 1H), 6.40 – 6.30 (m, 2H), 5.81 (dd, *J* = 9.2, 2.2 Hz, 1H), 4.62 (s, 15H), 3.96 (s, 3H), 3.81 (d, *J* = 6.3 Hz, 2H), 1.96 - 1.87 (m, 3H), 1.82- 1.73 (m, 3H), 1.39 - 1.19 (m, 3H), 1.08 (t, *J* = 11.9 Hz, 2H). ^{13}C NMR (101 MHz, $CDCl_3$) δ 169.80, 164.22, 153.89, 143.55, 136.60, 131.85, 126.75, 114.74, 107.48, 103.28, 74.59, 55.48, 37.22, 29.50, 26.10, 25.34.

Methyl 5-(hexyloxy)-4-methoxy-2-nitrobenzoate (2-2)—To a solution of methyl 5-hydroxy-4-methoxy-2-nitrobenzoate (227 mg, 1.0 mmol) in DMF (10 ml) was added K_2CO_3 (207 mg, 1.5 mmol) and bromohexane (198 mg, 1.2 mmol). The reaction mixture was

Author Manuscript Author Manuscript Author Manuscript Author Manuscript

heated to 100°C and stirred for 10 h. After the reaction was over, the mixture was cooled to RT. The mixture was then filtered to remove the inorganic material. The filtrate was diluted with water (5 ml) and extracted with ethyl acetate (3x10 ml). The combined organic layers were washed with water (3x10 mL) and dried over anhydrous sodium sulfate. Removal of solvent under vacuo gave the residue which was chromatographed on silica gel with EtOAc : Hexane (1:4 v/v) as eluent to give 286 mg (yield 92%) desired product. ^{1}H NMR (400 MHz, Chloroform-*d*) δ_H (ppm) = ^{1}H NMR (400 MHz, Chloroform-*d*) δ 7.45 (s, 1H), 7.05 (s, 1H), 4.09 (t, *J* = 6.8 Hz, 2H), 3.95 (s, 3H), 3.90 (s, 3H), 1.87 (p, *J* = 6.9 Hz, 2H), 1.45 (m, 2H), 1.34 (m, 4H), 0.95 – 0.86 (m, 3H).^{13}C NMR (101 MHz, $CDCl_3$) δ_C (ppm) = 166.61, 152.39, 150.65, 140.95, 121.85, 111.68, 107.22, 69.91, 56.68, 53.38, 31.57, 28.90, 25.62, 22.67, 14.14.

Methyl 2-amino-5-(hexyloxy)-4-methoxybenzoate (3-2)—To a solution of methyl 5-(hexyloxy)-4-methoxy-2-nitrobenzoate (250 mg, 0.80 mmol) in anhydrous MeOH was added Pd/C (10 wt%, 55 mg). The mixture was stirred under H_2 atmosphere for 4 h before it was filtered through a pad of celite. The solvent was removed in vacuo and the residue was purified by flash column chromatography to afford 202 mg (90%) of the desired product. ^{1}H NMR (400 MHz, Chloroform-*d*) δ_H (ppm) = 7.31 (s, 1H), 6.13 (s, 1H), 5.57 (br, 2H), 3.91 (t, *J* = 6.9 Hz, 2H), 3.84 (s, 6H), 1.79 (t, *J* = 7.6 Hz, 2H), 1.52 – 1.39 (m, 2H), 1.34 (m, 4H), 0.91 (d, *J* = 7.0 Hz, 3H). ^{13}C NMR (101 MHz, $CDCl_3$) δ_C (ppm) = 168.33, 155.56, 147.23, 140.08, 115.08, 102.30, 99.48, 70.06, 55.87, 51.44, 31.75, 29.38, 25.79, 22.79, 14.18.

Methyl 2-acrylamido-5-(hexyloxy)-4-methoxybenzoate (4-2)—Methyl 2-amino-5-(hexyloxy)-4-methoxybenzoate **(3-2)** (197 mg, 0.70 mmol) was dissolved in DCM (5 ml) followed by addition of acryloyl chloride (76 mg, 0.84 mmol) at 0°C. Triethylamine (84 mg, 0.84 mmol) was then syringed into the reaction mixture and the solution was stirred for 4 h and allowed to warm to RT. The reaction was concentrated and re-dissolved in EtOAc. The organic solution was then washed with water, saturated sodium bicarbonate, and brine. The organic layer was dried over magnesium sulfate, filtered, concentrated, and purified by column chromatography EtOAc : Hexanes (1:4) to deliver 211 mg (yield 90%) desired product. ^{1}H NMR (400 MHz, Chloroform-*d*) δ_H (ppm) = 11.40 (s, 1H), 8.57 (s, 1H), 7.47 (s, 1H), 6.58-6.23 (m, 2H), 5.77 (dd, *J* = 10.0, 1.4 Hz, 1H), 4.00 (t, *J* = 6.8 Hz, 2H), 3.96 (s, 3H), 3.90 (s, 3H), 1.83 (p, *J* = 7.0 Hz, 2H), 1.59 −1.38 (m, 2H), 1.40 - 1.21 (m, 4H), 1.02-0.77 (m, 3H). ^{13}C NMR (101 MHz, $CDCl_3$) δ_C (ppm) = 168.66, 164.18, 154.64, 143.64, 137.72, 132.52, 127.31, 113.99, 106.76, 103.68, 69.51, 56.23, 52.25, 31.71, 29.83, 29.22, 25.76, 22.71, 14.17.

2-Acrylamido-5-(hexyloxy)-4-methoxybenzoic acid (5-2, HJ-02)—Methyl 2-acrylamido-5-(hexyloxy)-4-methoxybenzoate (**4-2**) (20mg, 0.06 mmol) was dissolved in THF (1 ml) followed by 2M LiOH (0.12 ml, 0.24 mmol) and the mixture was stirred at r. t. overnight. After the reaction was over, acidify the mixture with 1N HCl and the product was extracted with ethyl acetate to afford 15 mg product. Yield: 80%.

^{1}H NMR (400 MHz, Methanol-d_4) δ_H (ppm) = 11.17 (s, 1H), 8.61 (d, *J* = 0.9 Hz, 1H), 7.55 (d, *J* = 1.0 Hz, 1H), 6.60-6.14 (m, 2H), 5.81 (dt, *J* = 10.0, 1.1 Hz, 1H), 4.03 (t, *J* = 6.8 Hz, 2H), 3.99 (s, 3H), 1.85 (p, *J* = 7.0 Hz, 2H), 1.60 −1.42 (m, 2H), 1.36 (m, 4H), 0.91 (t, *J*

Author Manuscript Author Manuscript Author Manuscript Author Manuscript

= 6.0Hz, 3H). ^{13}C NMR (101 MHz, $CDCl_3$) δ_C (ppm) = 172.36, 164.12, 155.51, 143.74, 138.38, 132.21, 127.67, 114.39, 105.45, 72.83, 69.37, 56.23, 31.58, 29.05, 25.63, 22.59, 14.05.

Methyl 5-(hex-5-yn-1-yloxy)-4-methoxy-2-nitrobenzoate (2-3)—To a solution of methyl 5-hydroxy-4-methoxy-2-nitrobenzoate (227 mg, 1.0 mmol) in DMF (10 ml) was added K_2CO_3 (207 mg, 1.5 mmol), KI (33 mg, 0.2 mmol) and 6-chloro-1-hexyne (140 mg, 1.2 mmol). The reaction mixture was heated to 120°C and stirred for 15 h. After the reaction was over, the mixture was cooled to RT. The mixture was then filtered to remove the inorganic material. Filtrate was diluted with water (5 ml) and extracted with ethyl acetate (3x10 ml). The combined organic layers were washed with water (3x10 ml) and dried over anhydrous sodium sulfate. Removal of solvent under vacuo gave the residue which was chromatographed on silica gel with EtOAc : Hexane (1:4 v/v) as eluent to give 270 mg (88%) desired product. ^{1}H NMR (400 MHz, Chloroform-*d*) δ 7.45 (s, 1H), 7.06 (s, 1H), 4.13 (t, *J* = 6.4 Hz, 2H), 3.95 (s, 3H), 3.90 (s, 3H), 2.29 (td, *J* = 7.0, 2.6 Hz, 2H), 2.12 – 1.89 (m, 3H), 1.80 – 1.63 (m, 2H). ^{13}C NMR (101 MHz, $CDCl_3$) δ 166.49, 152.15, 150.70, 141.13, 121.73, 111.75, 107.23, 83.82, 69.19, 69.07, 56.66, 53.37, 27.91, 24.88, 18.19.

Methyl 2-amino-5-(hex-5-yn-1-yloxy)-4-methoxybenzoate (3-3)—To a solution of methyl 5-(hex-5-yn-1-yloxy)-4-methoxy-2-nitrobenzoate (247 mg, 0.80 mmol) in anhydrous MeOH was added Pd/C (10 wt%, 55 mg). The mixture was stirred under H_2 atmosphere for 4 h before it was filtered through a pad of celite. The solvent was removed in vacuo and the residue was purified by flash column chromatography to afford 200 mg (90%) of the desired product. ^{1}H NMR (400 MHz, Chloroform-*d*) δ 7.32 (s, 1H), 6.13 (s, 1H), 5.58 (br, 2H), 3.96 (t, *J* = Hz, 2H), 3.84 (s, 6H), 2.28 (m, 2H), 1.99 – 1.85 (m, 3H), 1.73 (m, 2H). ^{13}C NMR (101 MHz, $CDCl_3$) δ 168.30, 155.64, 147.40, 139.93, 115.42, 102.30, 99.50, 84.36, 69.58, 68.68, 55.88, 51.47, 28.48, 25.20, 18.32.

Methyl 2-acrylamido-5- (hex-5-yn-1-yloxy)-4-methoxybenzoate (4-3)—Methyl 2-amino-5-(hex-5-yn-1-yloxy)-4-methoxybenzoate (4-2) (194 mg, 0.7 mmol) was dissolved in DCM (5 ml) followed by addition of acryloyl chloride (76 mg, 0.84 mmol) at 0 °C. Triethylamine (84 mg, 0.84 mmol) was then syringed into the reaction mixture and the solution was stirred for 4 h and allowed to warm to RT. The reaction was concentrated and re-dissolved in EtOAc. The organic solution was then washed with water, saturated sodium bicarbonate, and brine. The organic layer was dried over magnesium sulfate, filtered, concentrated, and purified by column chromatography (1:4) EtOAc:Hexanes) to deliver 207 mg (89%) desired product. ^{1}H NMR (400 MHz, Chloroform-*d*) δ 11.40 (s, 1H), 8.58 (s, 1H), 7.48 (s, 1H), 6.61 – 6.16 (m, 2H), 5.89 – 5.63 (m, 1H), 4.03 (t, *J* = 6.4 Hz, 2H), 3.96 (s, 3H), 3.91 (s, 3H), 2.29 (m, 2H), 1.97 (m, 3H), 1.81 – 1.68 (m, 2H). ^{13}C NMR (101 MHz, $CDCl_3$) δ 168.63, 164.23, 154.71, 143.50, 137.90, 132.51, 127.38, 114.30, 106.78, 103.74, 84.20, 68.89, 68.80, 56.24, 52.28, 28.30, 25.12, 18.30.

2-Acrylamido-5-(hex-5-yn-1-yloxy)-4-methoxybenzoic acid (5-3)—Methyl 2-acrylamido-5-(hex-5-yn-1-yloxy)-4-methoxybenzoate (**5-2**) was dissolved in THF (1ml) followed by 2 M LiOH (0.12 ml, 0.24 mmol) and the mixture was stirred overnight at RT.

Author Manuscript Author Manuscript Author Manuscript Author Manuscript

After the reaction was over, acidify the mixture with 1N HCl and the product was extracted with ethyl acetate to afford 16 mg product. Yield: 85%. ^{1}H NMR (400 MHz, Chloroform-*d*) δ 8.51 (s, 1H), 7.57 (s, 1H), 6.58 – 6.22 (m, 2H), 5.79 (dd, *J* = 9.8, 1.5 Hz, 1H), 4.06 (t, *J* = 6.5 Hz, 2H), 3.96 (s, 3H), 2.29 (td, *J* = 7.1, 2.7 Hz, 2H), 2.05 – 1.91 (m, 3H), 1.82 – 1.67 (m, 2H). ^{13}C NMR (101 MHz, $CDCl_3$) δ 170.28, 164.40, 154.26, 143.40, 137.32, 132.51, 127.30, 114.99, 107.56, 103.57, 84.08, 68.78, 68.69, 55.99, 28.13, 24.96, 18.11.

2-Acrylamido-4-methoxy-5-(octyloxy)benzoic acid (5-4)—Methyl 2-acrylamido-5-(octyloxy)-4-methoxy benzoate (4) was dissolved in THF (1 ml) followed by 2 M LiOH (0.12 ml, 0.24 mmol) and the mixture was stirred overnight at RT. After the reaction was over, acidify the mixture with 1N HCl and the product was extracted with ethyl acetate to afford 16 mg product. Yield: 85%. ^{1}H NMR (400 MHz, Chloroform-*d*) δ 11.19 (s, 1H), 8.61 (s, 1H), 7.54 (s, 1H), 6.46 – 6.28 (m, 2H), 5.81 (dd, *J* = 10.0, 1.4 Hz, 1H), 4.07 – 3.93 (m, 5H), 1.95 – 1.72 (m, 2H), 1.46 (m, 2H), 1.37 – 1.22 (m, 11H), 1.00 – 0.71 (m, 3H). ^{13}C NMR δ (101 MHz, $CDCl_3$) δ 171.79, 164.24, 155.58, 143.84, 138.53, 132.38, 127.74, 114.54, 105.52, 103.76, 69.53, 56.37, 31.95, 29.50, 29.36, 29.24, 26.09, 22.81, 14.27.

5-(cyclohexylmethoxy)-4-methoxy-2-propionamidobenzoic acid (5-5)—Methyl 5-(cyclohexylmethoxy)-4-methoxy-2-propionamidobenzoate was dissolved in THF (1ml) followed by 2 M LiOH (0.12 ml, 0.24 mmol) and the mixture was stirred overnight at RT.

Animals.

Pregnant Sprague Dawley rats were obtained from Jackson Laboratories West (Sacramento, CA). Rats were kept on a 12h:12h light-dark cycle with *ad libitum* access to food and water. Superior cervical ganglia from male and female neonatal rats were used for microfluidic explants and dissociated cultures. All procedures were approved by the OHSU Institutional Animal Care and Use Committee and comply with the Guide for the Care and Use of Laboratory Animals published by the National Academies Press (8th edition).

Sympathetic outgrowth assay.

Cultures of dissociated sympathetic neurons were prepared from superior cervical ganglia (SCG) of newborn rats as described [23]. Cells were pre-plated for 1 hour to remove non-neuronal cells, and then 5,000 neurons/well were plated onto a 96 well plate (TPP) coated with poly-L-lysine (PLL, 0.01%, Sigma-Aldrich) and either laminin (2 μg/mL, Trevigen) or laminin and CSPGs (1-2 μg/mL, Millipore; concentration was calibrated to inhibit outgrowth by 40-50% and differed between batches). Neurons were cultured in serum free C2 medium [24, 25] supplemented with 10 ng/mL NGF (Alomone Labs), 100 U/mL penicillin G, 100 μg/mL streptomycin sulfate (Invitrogen), and 2μM 5-Fluoro-2'-Deoxyuridine (Sigma). Neurons were treated with either vehicle (DMSO) or the compounds HJ-01, HJ-02, HJ-03, ISP or Illudalic acid at various concentrations as described in figure legends. Live-cell imaging was carried out using an Incucyte Zoom microscope (Essen BioScience), with 20x phase images acquired every 2 hrs over a 30 hr period. Neurite length was measured using Cell Player Neurotrack software (Essen BioScience) and used to calculate the neurite growth.

Author Manuscript Author Manuscript Author Manuscript Author Manuscript

Compartmentalized cultures.

Micro-fluidic chambers were generated by adding SYLGARD 184 silicone elastomer (Dow Corning) into a pre-cast mold, and heating at 50-60° C for 2 hours. Cleaned chambers were placed in 10 cm culture dishes (Corning) pre-coated with 0.01% PLL. The axonal compartment was then coated with 10 μg/mL collagen or collagen + 1 μg/mL CSPGs. SCG were placed in reduced growth factor Matrigel (BD Bioscience) within the cell body compartment. C2 media supplemented with 10 ng/mL NGF was added to both compartments and cultures were maintained at 37° C in a humidified 5% CO_2 incubator. After 24 hours, or when axons were first visible in the axonal compartment, images were acquired (t=0) and vehicle (5% DMSO), 100nM HJ-01, 100nM HJ-02, or 4μU/mL chondroitinase ABC were added to the axonal compartment. Additional images were obtained 3 hours later (t=3), and a growth rate was calculated based on the distance extended during that 3 hour period.

Western blotting.

Immunoblotting protein samples were prepared using 4x XT sample buffer and 20x XT reducing reagent (Biorad). Samples were boiled for 10 minutes at 95°C before being spun down and added to protein gels. To separate proteins by SDS-PAGE, Criterion pre-cast 4-12% gradient Bis-tris gels were used and run for 2 hours at 120V. Proteins were transferred to PVDF membranes by semi-dry transfer at 25V for 45 minutes. Protein laden PVDF membranes were blocked for 1 hour in 5% milk dissolved in TBST. Membranes were briefly rinsed with TBST and incubated with primary antibodies diluted in 5% BSA TBST for either 1 hour at room temperature or overnight at 4°C depending on the antibody. Following primary incubation blots were rinsed with TBST 3 times for 10 minutes each and placed in HRP-conjugated Igg secondary diluted in 5% milk TBST for 1 hour at room temperature. Blots were rinsed 3 times for 10 minutes each and imaged using SuperSignal HRP chemiluminescent substrate (ThermoFisher Scientific).

PTPσ D1 D2 protein purification.

D1D2 plasmid was a gift from (Brad Lang and Jerry Silver, Case Western Reserve University). Rosetta 2(DE3) competent cells (Novagen) were transformed with 1μL of D1D2 DNA and grown overnight at 37°C on LB agar plates supplemented with kanamycin and chloramphenicol. A ¼ swath of the bacteria from the LB agar plate was spiked into 50mL of LB media (with 50μg/mL kanamycin and 34μg/mL chloramphenicol) and grown at 37°C overnight with 225rpm shaking. The next day the 50mL starter culture was pitched into 1L of terrific broth (TB) media (12 g bacto tryptone, 24 g yeast extract, 0.4% glycerol, 17mM KH2PO4, 72mM K2HPO4, 1% glucose, 50 μg/ml Kanamycin, 34 μg/ml chloramphenicol) and grown at 37°C, 225rpm until reaching an OD600 reading of 0.6. At this point the TB media was placed on ice and the protein expression of D1D2 was induced with 0.4mM Isopropyl-β-thiogalactoside (IPTG, Sigma-Aldrich) and grown at 37°C overnight, 225rpm. Cells were harvested by centrifugation at 4000rpm 4°C for 15 min. The cell pellet was resuspended in 50mL of lysis buffer (20 mM HEPES, pH 7.5, 1 mM β-mercaptoethanol, 1 mM benzamidine, 0.2% NP-40, 0.2% Tween-20, 500 mM NaCl, 1 mM phenylmethylsulfonyl fluoride, 8.3 mg/L DNAse I) with a glass douncer and sonicated,

Author Manuscript Author Manuscript Author Manuscript Author Manuscript

on ice, 6 times for 30 seconds each time with 2 minutes rest between each cycle (Branson sonifier 450). The resulting lysate was cleared by centrifugation at 12,000 x G, 4°C, for 30 minutes. Purification of the D1D2 protein was achieved using the attached his-tag by Ni-NTA affinity chromatography (Ni-NTA resin, Qiagen). The resulting purified protein was verified by size using 10% SDS-PAGE before use in enzymatic activity assays.

PTPσ D1 D2 catalytic activity assessment.

The catalytic activity of purified PTPσ D1D2 catalytic domain was assessed using p-nitrophenyl phosphate (p-NPP, Sigma-aldrich), a commonly used indicator of phosphatase activity. D1D2 is capable of using p-NPP as a substrate and catalysis of the phosphate group results in a colorimetric reaction that can be monitored by 405nm absorbance. The assay was conducted in ice cold 50mM MES buffer with either 2mM or 10mM p-NPP. To this reaction mixture 30nM of D1D2 protein were added with either vehicle, 1μM HJ-02, or 12.5mM of sodium-orthovanadate (Sigma-Aldrich) as a control tyrosine phosphatase inhibitor. The reaction mixture was added to clear flat-bottom 96-well plates and kept on ice until the plate reading. A Spectra Max i3 (Molecular Devices) multi-well plate reader was used to measure 405nm absorbance. The reaction was induced by incubation at 30°C and measured continuously for 3 minutes.

Phosphatase Inhibition Assays.

The ability of compounds HJ-01, HJ-02, and Illudalic acid to inhibit a small panel of tyrosine phosphatase enzymes was investigated. The enzymes PTPσ, PTPRδ (protein tyrosine phosphatase receptor delta), LAR (leukocyte antigen-related tyrosine phosphatase), CD45 (cluster of differentiation antigen 45; also known as protein tyrosine phosphatase receptor C), SHP2 (Src homology 2 domain–containing phosphatase 2), and PTP1B (protein tyrosine phosphatase 1B) were incubated with 10 mM DTT for 30 min on ice in a buffer containing 50 mM HEPES pH 7.5, 100 mM NaCl, 1 mM EDTA, and 0.02% tween. The activity assays were performed in black 96-well plates in a total volume of 50 μL and 10% DMSO. The final concentration of enzyme in each reaction was180 pM for PTPσ, 9.7 nM for PTPRδ, 4.2 nM for LAR, 5 nM for CD45, 5 nM for SHP2, and 5 nM for PTP1B. Each enzyme was incubated with HJ-01 or HJ-02 for 30 min at 37°C, after which time the reaction was initiated by addition of the fluorogenic substrate DiFMUP to a final concentration of 30 μM. Enzyme activity was measured relative to an inhibitor-free control by monitoring the increase in fluorescence as DiFMUP was hydrolyzed to DiFMU. The fluorescence (λex = 350 nm, λem= 455 nm) was measured every 30 s for 30 min at 37°C. Each concentration was tested in triplicate.

Cell signaling.

TrkB-HEK-293t cells (a kind gift from Dr. Moses Chao, NYU) were used to examine the effects of HJ-01 and HJ-02 on TrkB stimulated ERK phosphorylation. Cells were plated on 6-well plates in HG-DMEM (Gibco) with 10%FBS (Hyclone), 1% Penicillin/streptomycin (Gibco) and Geniticin (400 μg/mL; Life Technologies). At the appropriate density cells with rinsed twice with 1x PBS and media was replaced with Opti-MEM (Gibco) containing 2%FBS. Cells were transfected with Lipofectamine 2000 (7μL per well) and with either 2.5μg full-length PTPσ plasmid or 1μg GFP control plasmid per well. After 6 hours cells

Author Manuscript Author Manuscript Author Manuscript Author Manuscript

were rinsed once with 1x PBS and replaced with regular growth media and grown for 12 hours. Cells were then serum starved for 2 hours in HG-DMEM + B27. Following serum starving cells were incubated with either HJ-01 or HJ-02 at 10nM, 100nM, or 1μM for 1 hour and then stimulated with 5ng/mL human BDNF (Alomone Labs) for 5 minutes. Cells were then rinsed with ice-cold PBS and lysed on ice with intermittent agitation for 30 minutes with Erk lysis buffer [50mM Tris (pH 8.0), 150mM NaCl, 2mM EDTA, 10mM NaF, 10% glycerol, and 1% NP-40] containing protease inhibitor cocktail (Roche), phosphatase inhibitor cocktails (Sigma), and 5mM iodoacetamide. Lysates sat on ice for 30min and were then treated with 10mM dithiothreitol to inactive any remaining iodoacetamide. Protein lysate was cleared by centrifugation at 13,000 x G for 10 minutes. The soluble fraction was removed and diluted with 4x XT sample buffer and 20x XT reducing reagent (Biorad) for western blot analysis as described above. Blots were probed with phospho-Erk1/2 (1:1000 Phospho-p44/42MAPK, Cell Signaling #9101) and Total-Erk1/2 (1:1000 p44/42MAPK, Cell Signaling #9102) antibodies.

Immunoprecipitation assay.

To test the hypothesis that small molecules HJ-01 and HJ-02 disrupt the binding of TrkA and PTPσ, HEK-293t cells were transfected with full length PTPσ or p75NTR (Addgene plasmid # 24091) and TrkA-RFP plasmid (Addgene plasmid #24093), and pulled down using RFP-trap nanobody conjugated to magnetic agarose (Chromotek). HEK-293t cells were plated onto 6-well plates coated with 0.01% poly-l-lysine (Sigma) in high-glucose DMEM (Gibco) supplemented with 10%FBS (Hyclone) and 1%Anti-Anti (Gibco). 12 hours later cells were rinsed with 1x PBS and media was replaced with Opti-MEM (Gibco) containing 2%FBS. Cells were transfected using Lipofectamine 3000 (Thermofisher Scientific). For transfection, 1μg of TrkA-RFP and 1μg of PTPσ plasmid, 6μL of P3000 reagent, and 5μL of lipofectamine reagent were added to each well of the 6-well plate. 12-16 hours later cells were rinsed twice with 1xPBS and media was replaced with DMEM and B27 supplement (Gibco) and serum starved for 4 hours. Cells were then treated with small molecules or vehicle (DMSO) for 1 hour and stimulated for an additional hour with 50ng/mL NGF (Alomone Labs #N-100) + 2μg/mL Chondroitin Sulfate Proteoglycans (EMD-Millipore CC117). Cells were rinsed twice with ice-cold 1x PBS and lysed with IP lysis buffer (150mM NaCl, 50mM Hepes, 1.5mM $MgCl_2$, 1mM EGTA, 1% Triton-X, 10% glycerol, 1x Roche complete protease inhibitor cocktail, and 1x Sigma phosphatase inhibitor cocktails 2 and 3). Two wells of each 6-well plate were pooled per condition, and cells were lysed for 30 minutes on ice with intermittent vortexing. Lysate was centrifuged at 13,000 x G for 10 minutes leaving the soluble fraction. 10% of this lysate was set aside as the input fraction. TrkA immunoprecipitation was accomplished using 15μL of RFP-trap magnetic agarose added to the remaining lysate and incubated overnight at 4°C on a rotator. The protein bound to the RFP-trap agarose was then separated using a magnet and rinsed 3 x 10 minutes. To remove the protein from the beads, 4x XT-sample buffer (Biorad) was diluted to 2x using the IP lysis buffer and XT reducing reagent was added the sample was then incubated at 95°C for 10 minutes and separated from the beads using a magnet. Samples were subjected to the standard western blotting protocol and probed for TrkA (1:1000; Millipore Sigma #06-574) and PTPσ (1:500; Proteintech #13008-1-AP) or, p75NTR (1:1000; Cell Signaling, D4B3 XP #8238S). To quantify pulldown of PTPσ (or

Author Manuscript Author Manuscript Author Manuscript Author Manuscript

p75NTR) by TrkA-RFP the levels of each protein in the pulldown were quantified by pixel density, normalized to the respective input levels and then the ratio of PTPσ (or p75NTR) to TrkA was calculated and compared across samples.

Statistics.

Data with multiple groups and one variable were analyzed by one-way ANOVA using either Dunnett or Tukey post-tests to control for multiple comparisons. Experiments with two variables were analyzed with two-way ANOVA using a Dunnett post-test. Statistical analyses were carried out using Prism version 8 or 9.

Supplementary Material

Refer to Web version on PubMed Central for supplementary material.

Acknowledgments:

The authors would like to thank Dr. Michael Pellegrino, Dr. Amber Bannon, Kimberly Vreugdenhil, Seongkyung Seo, and Antoinette Olivas for technical assistance with early studies of these compounds. We would like to thank Dr. Moses Chao (Skirball Institute, NYU) for the HEK-TrkB cells and for the TrkA-RFP and p75NTR plasmids (Addgene plasmid # 24093, 24091).

Funding Sources:

This work was supported by the Morton Cure Paralysis Fund, the OCTRI Biomedical Innovation Program, the OHSU Bioscience Innovation Program, and the M.J. Murdock Charitable Trust (MSC & BAH); NIH R01 HL093056 (BAH); NIH GM135295 (AMB); NIH P20GM103434 via the West Virginia IDeA Network for Biomedical Research Excellence (GBD); NIH T32HL094294 and AHA 19POST34460031 (RTG); NIH F31HL152490, AHA 20PRE35210768 and the Steinberg Endowment for Graduate Education (MRB).

Data Availability:

The datasets generated during and/or analyzed during the current study are available from the corresponding author on reasonable request.

Abbreviations:

CSPG	Chondroitin Sulfate Proteoglycan
PTPσ/PTPrs	Protein Tyrosine Phosphatase receptor sigma
Trk	Tropomyosin-receptor kinase

References

1. Bradbury EJ; Moon LD; Popat RJ; King VR; Bennett GS; Patel PN; Fawcett JW; McMahon SB, Chondroitinase ABC promotes functional recovery after spinal cord injury. Nature. 2002, 416 (6881), 636–640. [PubMed: 11948352]
2. Tom VJ; Sandrow-Feinberg HR; Miller K; Domitrovich C; Bouyer J; Zhukareva V; Klaw MC; Lemay MA; Houle JD, Exogenous BDNF enhances the integration of chronically injured axons that regenerate through a peripheral nerve grafted into a chondroitinase-treated spinal cord injury site. Exp.Neurol 2013, 239:91–100. doi: 10.1016/j.expneurol.2012.09.011. Epub@2012 Sep 27., 91-100. [PubMed: 23022460]

Author Manuscript Author Manuscript Author Manuscript Author Manuscript

3. Tom VJ; Kadakia R; Santi L; Houle JD, Administration of chondroitinase ABC rostral or caudal to a spinal cord injury site promotes anatomical but not functional plasticity. J.Neurotrauma 2009, 26 (12), 2323–2333. [PubMed: 19659409]

4. Zhao RR; Muir EM; Alves JN; Rickman H; Allan AY; Kwok JC; Roet KC; Verhaagen J; Schneider BL; Bensadoun JC; Ahmed SG; Yanez-Munoz RJ; Keynes RJ; Fawcett JW; Rogers JH, Lentiviral vectors express chondroitinase ABC in cortical projections and promote sprouting of injured corticospinal axons. J.Neurosci.Methods 2011, 201 (1), 228–238. [PubMed: 21855577]

5. Shen Y; Tenney AP; Busch SA; Horn KP; Cuascut FX; Liu K; He Z; Silver J; Flanagan JG, PTPsigma is a receptor for chondroitin sulfate proteoglycan, an inhibitor of neural regeneration. Science. 2009, 326 (5952), 592–596. [PubMed: 19833921]

6. Fry EJ; Chagnon MJ; Lopez-Vales R; Tremblay ML; David S, Corticospinal tract regeneration after spinal cord injury in receptor protein tyrosine phosphatase sigma deficient mice. Glia. 2010, 58 (4), 423–433. [PubMed: 19780196]

7. Gardner RT; Habecker BA, Infarct-derived chondroitin sulfate proteoglycans prevent sympathetic reinnervation after cardiac ischemia-reperfusion injury. J Neurosci 2013, 33 (17), 7175–83. [PubMed: 23616527]

8. Lang BT; Cregg JM; DePaul MA; Tran AP; Xu K; Dyck SM; Madalena KM; Brown BP; Weng YL; Li S; Karimi-Abdolrezaee S; Busch SA; Shen Y; Silver J, Modulation of the proteoglycan receptor PTPsigma promotes recovery after spinal cord injury. Nature 2015, 518 (7539), 404–8. [PubMed: 25470046]

9. Gardner RT; Wang L; Lang BT; Cregg JM; Dunbar CL; Woodward WR; Silver J; Ripplinger CM; Habecker BA, Targeting protein tyrosine phosphatase sigma after myocardial infarction restores cardiac sympathetic innervation and prevents arrhythmias. Nature communications 2015, 6, 6235.

10. Xie Y; Massa SM; Ensslen-Craig SE; Major DL; Yang T; Tisi MA; Derevyanny VD; Runge WO; Mehta BP; Moore LA; Brady-Kalnay SM; Longo FM, Protein-tyrosine phosphatase (PTP) wedge domain peptides: a novel approach for inhibition of PTP function and augmentation of protein-tyrosine kinase function. J Biol.Chem 2006, 281 (24), 16482–16492. [PubMed: 16613844]

11. Faux C; Hawadle M; Nixon J; Wallace A; Lee S; Murray S; Stoker A, PTPsigma binds and dephosphorylates neurotrophin receptors and can suppress NGF-dependent neurite outgrowth from sensory neurons. Biochim Biophys Acta 2007, 1773 (11), 1689–700. [PubMed: 17967490]

12. Ling Q; Huang Y; Zhou Y; Cai Z; Xiong B; Zhang Y; Ma L; Wang X; Li X; Li J; Shen J, Illudalic acid as a potential LAR inhibitor: Synthesis, SAR, and preliminary studies on the mechanism of action. Bioorganic & Medicinal Chemistry 2008, 16 (15), 7399–7409. [PubMed: 18579388]

13. McCullough BS; Batsomboon P; Hutchinson KB; Dudley GB; Barrios AM, Synthesis and PTP Inhibitory Activity of Illudalic Acid and Its Methyl Ether, with Insights into Selectivity for LAR PTP over Other Tyrosine Phosphatases under Physiologically Relevant Conditions. J Nat Prod 2019, 82 (12), 3386–3393. [PubMed: 31809044]

14. Fulo HF; Rueb NJ; Gaston R Jr.; Batsomboon P; Ahmed KT; Barrios AM; Dudley GB, Synthesis of illudalic acid and analogous phosphatase inhibitors. Org Biomol Chem 2021, 19 (48), 10596–10600. [PubMed: 34847212]

15. Sapieha PS; Duplan L; Uetani N; Joly S; Tremblay ML; Kennedy TE; Di Polo A, Receptor protein tyrosine phosphatase sigma inhibits axon regrowth in the adult injured CNS. Molecular and Cellular Neuroscience 2005, 28 (4), 625–635. [PubMed: 15797710]

16. Boutselis IG; Yu X; Zhang ZY; Borch RF, Synthesis and cell-based activity of a potent and selective protein tyrosine phosphatase 1B inhibitor prodrug. J Med Chem 2007, 50 (4), 856–64. [PubMed: 17249650]

17. Sherman LS; Back SA, A 'GAG' reflex prevents repair of the damaged CNS. Trends Neurosci. 2008, 31 (1), 44–52. [PubMed: 18063497]

18. Coles CH; Shen Y; Tenney AP; Siebold C; Sutton GC; Lu W; Gallagher JT; Jones EY; Flanagan JG; Aricescu AR, Proteoglycan-Specific Molecular Switch for RPTPσ Clustering and Neuronal Extension. Science 2011, 332 (6028), 484–488. [PubMed: 21454754]

19. Zaro BW; Vinogradova EV; Lazar DC; Blewett MM; Suciu RM; Takaya J; Studer S; de la Torre JC; Casanova JL; Cravatt BF; Teijaro JR, Dimethyl Fumarate Disrupts Human Innate Immune

Author Manuscript Author Manuscript Author Manuscript Author Manuscript

Signaling by Targeting the IRAK4-MyD88 Complex. Journal of immunology (Baltimore, Md. : 1950) 2019, 202 (9), 2737–2746.

20. Ohtake Y; Saito A; Li S, Diverse functions of protein tyrosine phosphatase σ in the nervous and immune systems. Exp Neurol 2018, 302, 196–204. [PubMed: 29374568]
21. Luo F; Tran AP; Xin L; Sanapala C; Lang BT; Silver J; Yang Y, Modulation of proteoglycan receptor PTPsigma enhances MMP-2 activity to promote recovery from multiple sclerosis. Nature communications 2018, 9 (1), 4126.
22. Pu A; Stephenson EL; Yong VW, The extracellular matrix: Focus on oligodendrocyte biology and targeting CSPGs for remyelination therapies. Glia 2018, 66 (9), 1809–1825. [PubMed: 29603376]
23. Dziennis S; Habecker BA, Cytokine suppression of dopamine-beta-hydroxylase by extracellular signal-regulated kinase-dependent and -independent pathways. The Journal of biological chemistry 2003, 278 (18), 15897–904. [PubMed: 12609984]
24. Lein P; Johnson M; Guo X; Rueger D; Higgins D, Osteogenic protein-1 induces dendritic growth in rat sympathetic neurons. Neuron 1995, 15 (3), 597–605. [PubMed: 7546739]
25. Pellegrino MJ; Parrish DC; Zigmond RE; Habecker BA, Cytokines inhibit norepinephrine transporter expression by decreasing Hand2. Mol Cell Neurosci 2011, 46 (3), 671–80. [PubMed: 21241805]

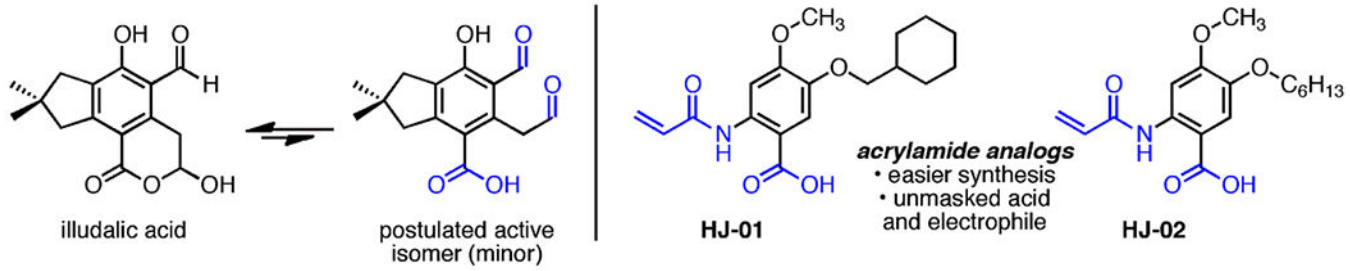

Figure 1.

Structures of HJ-01 and HJ-02 and the natural product that inspired their design, Illudalic acid. For full synthesis scheme and chemical products, refer to Supplemental Scheme 1. The unmasked acid and electrophiles (bis-aldehyde for illudalic acid and acrylamide for HJ-01/2) are in blue.

Author Manuscript Author Manuscript Author Manuscript Author Manuscript

Author Manuscript Author Manuscript Author Manuscript Author Manuscript

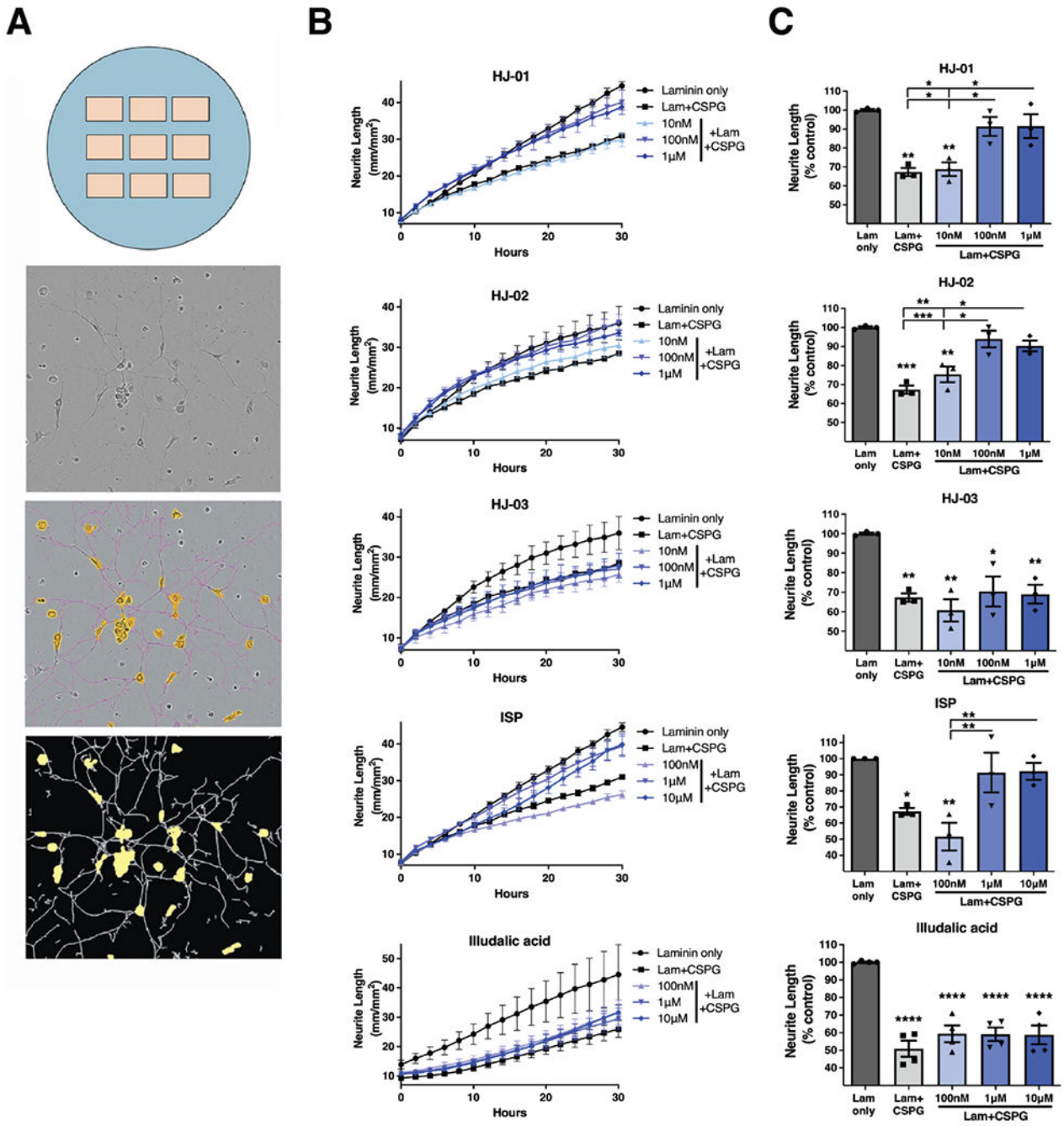

Figure 2. Compounds restore sympathetic neurite outgrowth over CSPGs *in vitro*.

(A) Illustration of a single well, the 9 fields of view/well that were photographed repeatedly, and a representative phase image of dissociated sympathetic neurons. Neurons are "masked" by the NeuroTrack software, cell bodies (yellow) and neurites (purple) are identified, and neurite length normalized to cell body area is calculated by the software. **(B, C)** Quantification of sympathetic neurite growth on Laminin only or Laminin and CSPGs in the presence of vehicle (5% DMSO), HJ-01, HJ-02, HJ-03, ISP, or Illudalic acid. **(B)** Representative growth curves from individual experiments are mean neurite length ± SEM

Author Manuscript Author Manuscript Author Manuscript Author Manuscript

of 9 locations/well and 3 wells per condition. Similar results were obtained in at least 3 independent experiments. **(C)** Data shown are the average of at least 3 experiments expressed as a percent of laminin-only vehicle (5% DMSO) treated controls; mean neurite length ± SD. Statistics: one-way ANOVA (Tukey's post-test), comparisons are to Laminin only control unless indicated by brackets *p<.05, **p<.01, ***p<0.001, ****p<0.0001.

Author Manuscript Author Manuscript Author Manuscript Author Manuscript

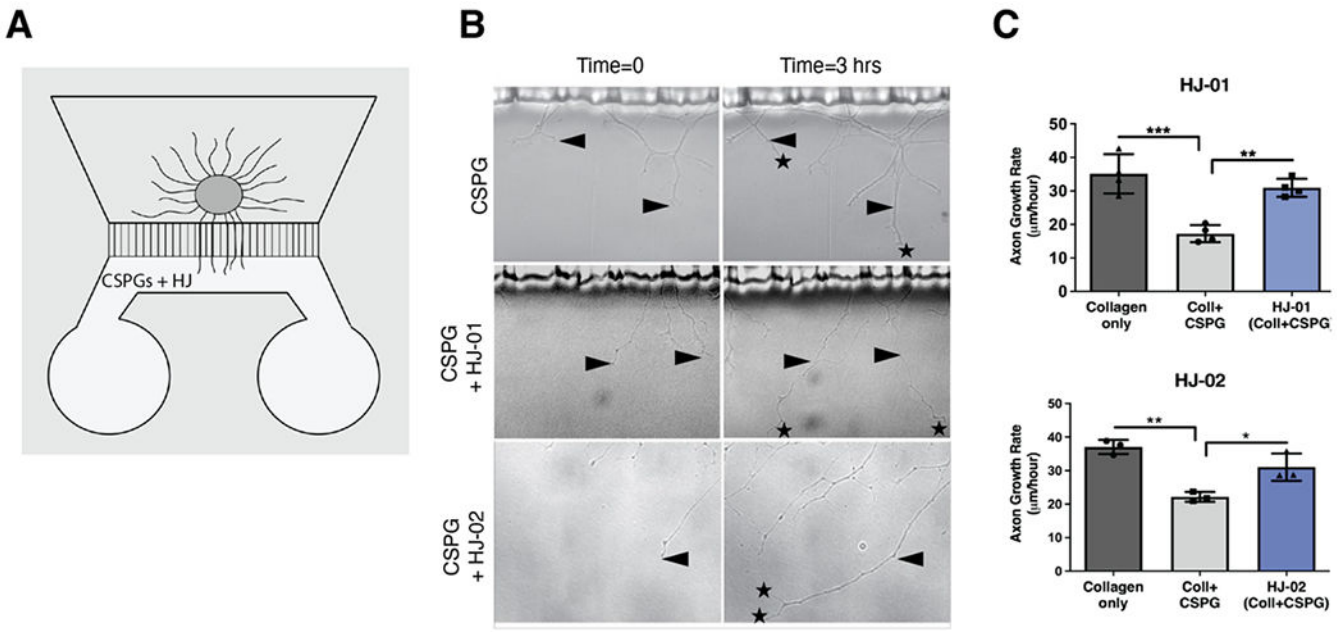

Figure 3. Axonal application of HJ-01 and HJ-02 is sufficient to promote sympathetic axon growth over CSPGs

(A) Illustration of microfluidic chambers, where whole ganglia are cultured in the cell body compartment and axons extend into the coated compartment where treatments are added to the media. **(B)** Representative images of axons in microfluidic chambers coated with CSPGs, taken at t=0 and t=3 hrs. Axons were treated with vehicle (5% DMSO), 100nM compound HJ-01, or HJ-02. Triangles identify the leading edge of the axon at t=0, and the asterisks identify the final position of the axon at t=3 hrs. **(C)** Quantification of axon growth rate in microfluidic chambers across collagen-only treated with vehicle, collagen and CSPGs treated with vehicle or, collagen and CSPGs treated with HJ-01 or HJ-02. Data are mean ± SEM of at least 8 axons per conditions across 3 separate experiments. Statistics; one-way ANOVA, (Tukey's post-test), Comparisons directly to collagen + CSPG treated samples, *p<.05, **p<.01, ***p<0.001.

Author Manuscript
Author Manuscript
Author Manuscript
Author Manuscript

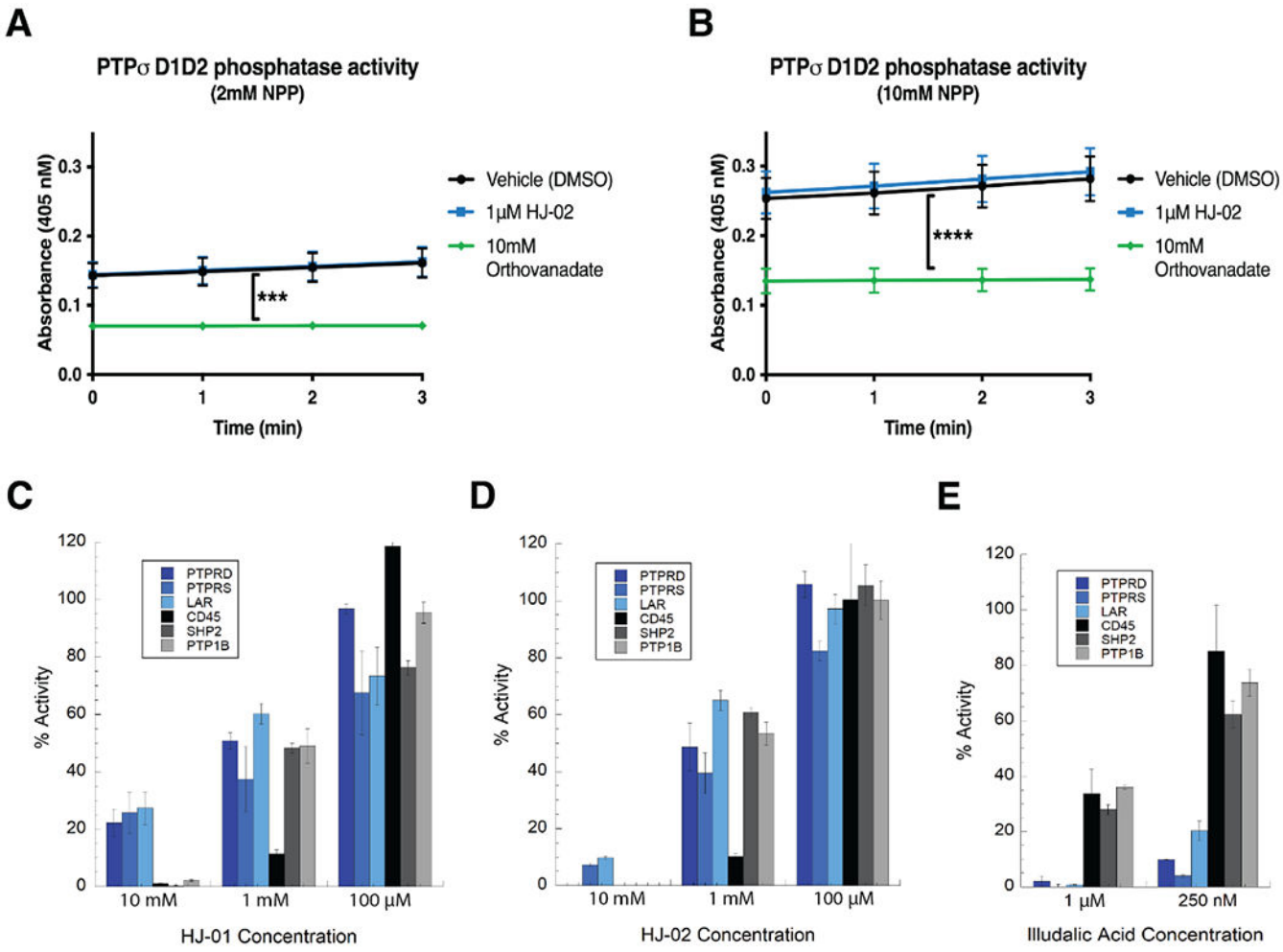

Figure 4. HJ-01 and HJ-02 do not inhibit PTPσ phosphatase activity at biologically relevant concentrations.

(A,B) PTPσ phosphatase activity was quantified in the presence of 1μM HJ-02 using purified PTPσ D1D2 phosphatase domain. HJ-02 did not inhibit D1D2 phosphatase activity at any time point or substrate concentration, while the phosphatase inhibitor orthovanadate significantly reduced phosphatase activity at all times and substrate concentrations. Data are absorbance at 405nm mean ± SD, n=3 experiments, ***p<0.001, ****p<0.0001, two-way ANOVA (Dunnett multiple comparisons test). **(C-E)** PTP protein family members were screened to examine the ability of HJ-01 (C), HJ-02 (D), or Illudalic Acid (E) to inhibit enzymatic activity; PTPRδ (PTPRD, dark blue), PTPσ (PTPRS, blue), LAR (light blue), CD45 (black), SHP2 (dark grey), and PTP1B (light grey). Data are mean ± SEM of three independent experiments.

Author Manuscript Author Manuscript Author Manuscript Author Manuscript

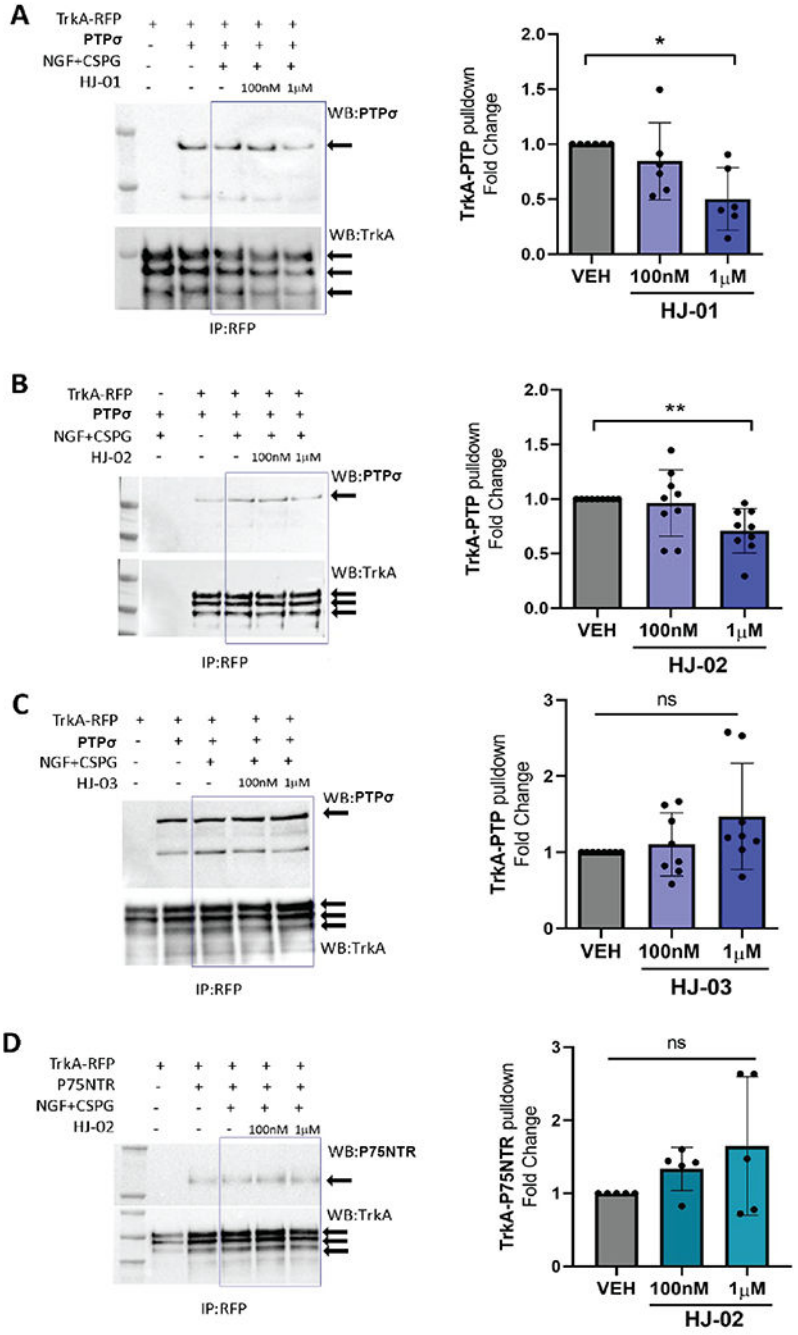

Figure 5. HJ-01and HJ-02 reduce the interaction between PTPσ and TrkA.

Representative western blots **(left)** probing for PTPσ and TrkA following TrkA-RFP immunoprecipitation. HEK-293t cells were transfected with TrkA-RFP and PTPσ, treated with either vehicle (DMSO), **(A)** HJ-01, **(B)** HJ-02, or **(C)** HJ-03 then stimulated with CSPGs and NGF. Quantification **(right)** of PTPσ that co-immunoprecipitated with TrkA-RFP normalized to vehicle treated cells. HJ-01 and HJ-02 reduced the amount of PTPσ that bound to TrkA-RFP at 1μM, but HJ-03 had no effect. **(D)** HEK-293t cells were transfected with TrkA-RFP and p75NTR, treated with vehicle (DMSO) and HJ-02, then stimulated

Author Manuscript Author Manuscript Author Manuscript Author Manuscript

with CSPGs and NGF. Quantification **(right)** of p75NTR that co-immunoprecipitated with TrkA-RFP normalized to vehicle treated cells. Data are mean ± SD, n=5-9 experiments; n.s.- not significant, *p<.05, **p<.01 vs. vehicle treated control, one-way ANOVA (Dunnett multiple comparisons post-test).

Author Manuscript Author Manuscript Author Manuscript Author Manuscript

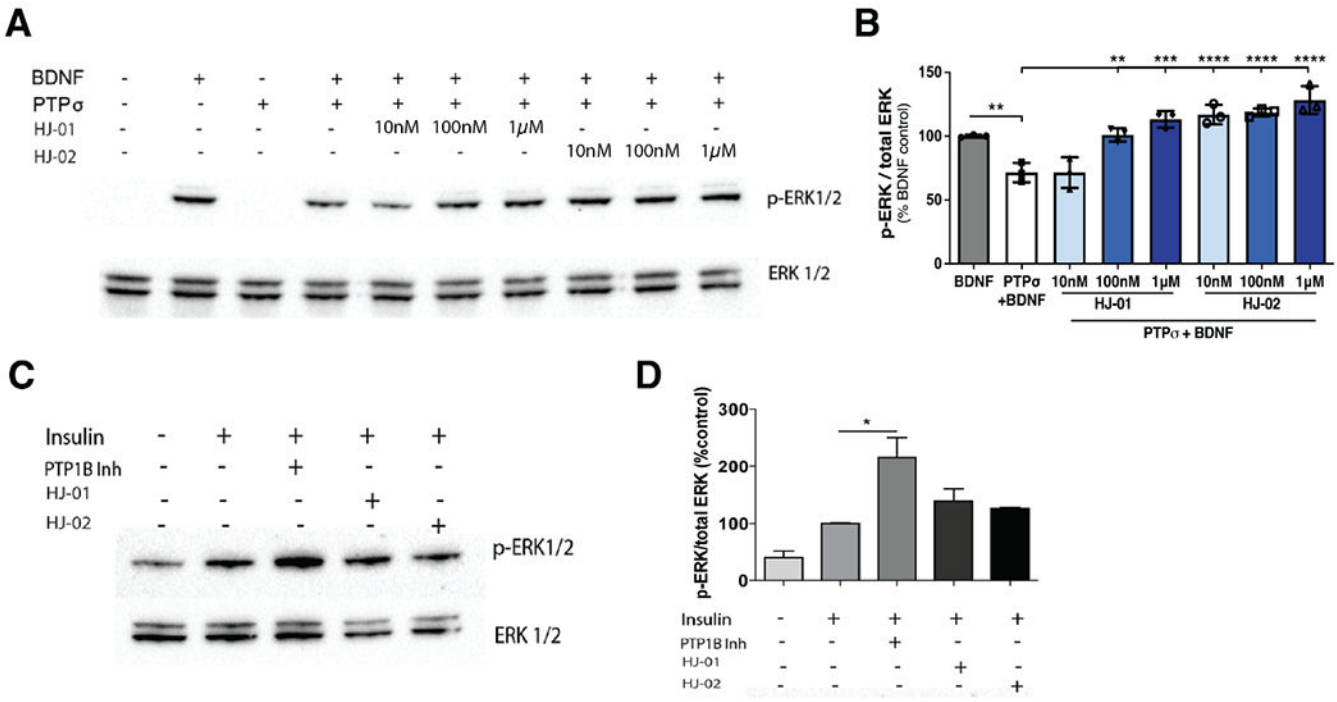

Figure 6. HJ-01 and HJ-02 block PTPσ reduction in TrkB signaling

(A) Representative Western blot of TrkB downstream signaling in the presence of PTPσ. Addition of PTPσ decreased BDNF-stimulated ERK1/2 phosphorylation. Both HJ-01 and HJ-02 restored ERK1/2 phosphorylation in response to BDNF. **(B)** Quantification of Phospho-ERK1/2 relative to Total-ERK1/2. Data are graphed as percent of vehicle control (BDNF stimulated cells); mean ± SD, n=3 experiments, ***p<0.001, ****p<0.0001 as noted by lines, one-way ANOVA (Tukey multiple comparisons test). **(C,D)** Western blot analysis examining potential effect of HJ-01 or HJ-02 on PTP1B/IR- β signaling in response to insulin. Mean ± SD, n=3 experiments, *p<0.05 vs. insulin control, one-way ANOVA, (Tukey multiple comparisons test).